Resonance families and their action on betatron motion

G. De Ninno[1] and D. Fanelli[2]

[1]*CERN PS/HP, 1211 Geneve 23, Switzerland*

[2]*Department of Numerical Analysis and Computer Science, KTH, S-100 44 Stockholm, Sweden*

The present paper takes one step beyond the single-resonance theory for betatron motion by summing all the members of a given resonance family and expressing the joint influence in a single driving term. As a demonstration and confirmation of this work, the family driving terms are used to derive the classic closed-orbit and betatron-modulation equations of Courant and Snyder. A more serious demonstration is made by applying the family driving terms to the compensation of linear coupling and showing how numerical matrix-based and resonance compensation schemes are related. In a final phase, the Hénon map is used to compare the efficiency of different coupling compensation schemes with respect to dynamic aperture.

PACS numbers: 41.85.–p, 29.27.–a

I. INTRODUCTION

Transverse, single-particle dynamics in synchrotrons has been widely studied using a Hamiltonian treatment in which the perturbation terms for single resonances are retained with the basic stable motion. These studies refer back to the classic references [1–4]. The action of single resonances has been successfully applied to the case of half and third integer extraction [5] and more general phenomena such as the beam losses in the CERN Intersecting Storage Rings [6]. The present paper takes one further step in showing that the influence of all the resonances in a particular family can be summed and that their combined driving term can be used to derive well-known equations such as the closed-orbit distortion equation of Courant and Snyder [7]. The application of the summed driving terms is taken further and used to make an analytical bridge between the coupling compensation schemes that have, in the past, been based on single coupling resonances and the numerical approach of arranging the off-axis blocks in the 4×4 transfer matrix to be zero.

II. THE SUMMED-RESONANCE DRIVING TERM

The summed-resonance driving term $C_{n_1,n_2,\infty}$ of a given resonance of order $N = n_1 + n_2$ can be calculated by summing the single-resonance driving term $C_{n_1,n_2,p}$ [8] over all the p harmonics[1]:

$$C_{n_1,n_2,\infty} = \sum_{p=-\infty}^{+\infty} C_{n_1,n_2,p} \,. \quad (1)$$

Expressing (1) explicitly one has

$$C_{n_1,n_2,\infty} = \sum_{p=-\infty}^{\infty} \int_0^{2\pi} A(\theta) e^{-i(n_1 Q_x + n_2 Q_y - p)\theta} \, d\theta \,, \quad (2)$$

where

$$
\begin{aligned}
A(\theta) = {} & \frac{R^2}{\pi (2R)^{N/2} |n_1|! \, |n_2|!} \beta_x(\theta)^{|n_1|/2} \beta_y(\theta)^{|n_2|/2} \\
& \times e^{i[n_1 \mu_x(\theta) + n_2 \mu_y(\theta)]} \bar{K}(\theta) \,,
\end{aligned}
\quad (3)
$$

with,[2] in the most common case,

$$
\begin{aligned}
\bar{K} = {} & (-1)^{(|n_2|+2)/2} \frac{1}{|B\rho|} \\
& \times \left[\left(\frac{\partial^{N-1} B_y}{\partial x^{N-1}} \right) + \frac{B_s}{2} \left(|n_1| \frac{\alpha_x}{\beta_x} - |n_2| \frac{\alpha_y}{\beta_y} \right) \right. \\
& \left. - i \frac{B_s}{2} \left(\frac{n_1}{\beta_x} - \frac{n_2}{\beta_y} \right) \right],
\end{aligned}
$$

for $|n_2|$ even, and

$$
\begin{aligned}
\bar{K} = {} & (-1)^{(|n_2|-1)/2} \frac{1}{|B\rho|} \\
& \times \left[\left(\frac{\partial^{N-1} B_x}{\partial x^{N-1}} \right) + \frac{B_s}{2} \left(|n_1| \frac{\alpha_x}{\beta_x} - |n_2| \frac{\alpha_y}{\beta_y} \right) \right. \\
& \left. - i \frac{B_s}{2} \left(\frac{n_1}{\beta_x} - \frac{n_2}{\beta_y} \right) \right],
\end{aligned}
$$

for $|n_2|$ odd.

The terms containing the axial field B_s in the two previous formulas have to be considered only if $n_1 = 1$, $n_2 = \pm 1$ (linear coupling). A more general expression for $\bar{K}$ that allows the presence of a varying axial field to be taken into account (and does not include the linear case) is given by

---

[1]Note that although Eq. (1) is expressed in the resonance form, it is valid whether the exponent is small or not, which is why one can meaningfully sum over p.

[2]In the following formulas the partial derivatives are evaluated at $x = y = 0$.

$$\bar{K} = (-1)^{(|n_2|+2)/2} \frac{1}{2|B\rho|} \left[(-1)^{(|n_2|+2)/2} \left(\frac{\partial^{(N-1)}B_y}{\partial x^{(N-|n_2|-2)}\partial y^{(|n_2|+1)}} - \frac{\partial^{(N-1)}B_x}{\partial x^{(N-|n_2|-1)}\partial y^{|n_2|}} \right) \right.$$

$$\left. + \frac{\partial^{(N-2)}B_s}{\partial x^{(N-|n_2|-2)}\partial y^{|n_2|}} \left(|n_1|\frac{\alpha_x}{\beta_x} - |n_2|\frac{\alpha_y}{\beta_y} \right) - i\frac{\partial^{(N-2)}B_s}{\partial x^{(N-|n_2|-2)}\partial y^{|n_2|}} \left(\frac{n_1}{\beta_x} - \frac{n_2}{\beta_y} \right) \right],$$

for $|n_2|$ even, $N \geq 3$ and $1 \leq |n_2| \leq (N-2)$;

$$\bar{K} = (-1)^{(|n_2|-1)/2} \frac{1}{2|B\rho|} \left[(-1)^{(|n_2|-1)/2} \left(\frac{\partial^{(N-1)}B_y}{\partial x^{(N-|n_2|-2)}\partial y^{(|n_2|+1)}} - \frac{\partial^{(N-1)}B_x}{\partial x^{(N-|n_2|-1)}\partial y^{|n_2|}} \right) \right.$$

$$\left. + \frac{\partial^{(N-2)}B_s}{\partial x^{(N-|n_2|-2)}\partial y^{|n_2|}} \left(|n_1|\frac{\alpha_x}{\beta_x} - |n_2|\frac{\alpha_y}{\beta_y} \right) - i\frac{\partial^{(N-2)}B_s}{\partial x^{(N-|n_2|-2)}\partial y^{|n_2|}} \left(\frac{n_1}{\beta_x} - \frac{n_2}{\beta_y} \right) \right],$$

for $|n_2|$ odd, $N \geq 3$ and $1 \leq |n_2| \leq (N-2)$.

The angle $\theta = s/R$ is the coordinate along the ring, $Q_{x,y}$ are the horizontal and vertical tunes, $\mu_{x,y}$ are the horizontal and vertical phase advances, $\beta_{x,y}$ are the horizontal and vertical beta functions, and R is the average radius of the ring. Suppose $\bar{K}(\theta)$ is different from zero and constant in j short intervals (i.e., the regions occupied by the sources of coupling and by possible correctors) $[\theta_i, \theta_i + \Delta\theta_i]$ in which $A(\theta)$ can be considered approximately constant (thin lens approximation)[3]:

$$C_{n_1,n_2,\infty} = \sum_{i=1}^{j} (\Delta C_{n_1,n_2,\infty})_i. \tag{4}$$

Now define $\Delta \equiv n_1 Q_x + n_2 Q_y$ and compute $(\Delta C_{n_1,n_2,\infty})_i$,

the contribution to $C_{n_1,n_2,\infty}$ from the ith subelement,

$$(\Delta C_{n_1,n_2,\infty})_i = \sum_{p=-\infty}^{+\infty} \int_{\theta_i}^{\theta_i+\Delta\theta_i} A(\theta)e^{-i[\Delta-p]\theta}\,d\theta, \tag{5}$$

which, when integrated, gives

$$(\Delta C_{n_1,n_2,\infty})_i \simeq A(\theta_i) \sum_{p=-\infty}^{+\infty} \frac{i}{\Delta-p} [e^{-i[\Delta-p](\theta_i+\Delta\theta_i)} - e^{-i[\Delta-p]\theta_i}]. \tag{6}$$

The summation can be redefined making use of the shift $[\Delta]$ (the closest integer to Δ) so that $p = [\Delta] + k$ where k is an integer. In the limit $(\Delta - [\Delta])\Delta\theta_i \ll 1$, the previous expression becomes[4]

$$(\Delta C_{n_1,n_2,\infty})_i \simeq A(\theta_i)e^{-i(\Delta-[\Delta])\theta_i} \sum_{k=-\infty}^{+\infty} \frac{i}{(\Delta-[\Delta])-k} [e^{ik(\theta_i+\Delta\theta_i)} - e^{ik\theta_i}]$$

$$= A(\theta_i)e^{-i(\Delta-[\Delta])\theta_i} \sum_{k=-\infty}^{+\infty} \frac{1}{(\Delta-[\Delta])-k} \left(\sin(k\theta_i) - \sin[k(\theta_i+\Delta\theta_i)] \right.$$

$$\left. + i\{\cos[k(\theta_i+\Delta\theta_i)] - \cos(k\theta_i)\} \right). \tag{7}$$

To sum these series first rewrite them in a more suitable form ($x = \theta_i$ or $x = \theta_i + \Delta\theta_i$) valid when $0 < x < 2\pi$ [9]:

$$\sum_{k=-\infty}^{+\infty} \frac{\sin(kx)}{(\Delta-[\Delta])-k} = -\frac{\pi \sin[(\Delta-[\Delta])(\pi-x)]}{\sin[(\Delta-[\Delta])\pi]}, \tag{8}$$

$$\sum_{k=-\infty}^{+\infty} \frac{\cos(kx)}{(\Delta-[\Delta])-k} = \frac{\pi \cos[(\Delta-[\Delta])(\pi-x)]}{\sin[(\Delta-[\Delta])\pi]}. \tag{9}$$

The application of (8) and (9) to (7) then gives

$$(\Delta C_{n_1,n_2,\infty})_i = A(\theta_i)e^{-i(\Delta-[\Delta])\theta_i}\frac{\pi}{\sin[(\Delta-[\Delta])\pi]} \left(\sin[(\Delta-[\Delta])(\pi-\theta_i-\Delta\theta_i)] - \sin[(\Delta-[\Delta])(\pi-\theta_i)] \right.$$

$$\left. + i\{\cos[(\Delta-[\Delta])(\pi-\theta_i-\Delta\theta_i)] - \cos[(\Delta-[\Delta])(\pi-\theta_i)]\} \right)$$

$$= -A(\theta_i)e^{-i(\Delta-[\Delta])\theta_i}\frac{2\pi}{\sin[(\Delta-[\Delta])\pi]} \sin\left[(\Delta-[\Delta])\frac{\Delta\theta_i}{2} \right] e^{-i[(\Delta-[\Delta])(\pi-\theta_i-\Delta\theta_i/2)]}. \tag{10}$$

---

[3]In a real machine $A(\theta)$ will vary slowly, or, at least, it will be possible to cut the elements into short enough pieces that $A(\theta)$ can be considered as constant over all subelements to any desired degree of accuracy.

[4]In the expression (7) the term $e^{-i(\Delta-[\Delta])\Delta\theta}$ is expanded to the zeroth order while the terms $e^{ik\Delta\theta}$ with $k \simeq (\Delta-[\Delta])$ are not expanded. This assumption is supported *a posteriori* by the accuracy of the final result.

After expressing $A(\theta_i)$ explicitly, $(\Delta C_\infty)_i$ becomes

$$
(\Delta C_{n_1,n_2,\infty})_i \simeq -\frac{R^2 \bar{K}_i}{(2R)^{N/2}|n_1|!\,|n_2|!} \frac{(\Delta - [\Delta])\Delta\theta_i}{\sin[(\Delta - [\Delta])\pi]}
$$
$$
\times \beta_x(\theta_i)^{|n_1|/2}\beta_y(\theta_i)^{|n_2|/2}
$$
$$
\times e^{i[n_1\mu_x(\theta_i)+n_2\mu_y(\theta_i)-(\Delta-[\Delta])\pi]}. \qquad (11)
$$

Equation (11) can be summed directly for all the elementary elements in the ring to give the coupling coefficient $C_{n_1,n_2,\infty}$ for the combined influence of the resonance family:

$$
C_{n_1,n_2,\infty} = -\frac{\pi(\Delta - [\Delta])}{\sin[\pi(\Delta - [\Delta])]} \frac{R^2}{\pi(2R)^{N/2}|n_1|!\,|n_2|!}
$$
$$
\times \int_0^{2\pi} \beta_x^{|n_1|/2}\beta_y^{|n_2|/2}
$$
$$
\times e^{i[n_1\mu_x+n_2\mu_y-(\Delta-[\Delta])\pi]}\bar{K}\,d\theta. \qquad (12)
$$

The basic differences between the summed-resonance driving term and the standard- (single-) resonance driving term [8]

$$
C_{n_1,n_2,p} = \frac{R^2}{\pi(2R)^{N/2}|n_1|!\,|n_2|!}
$$
$$
\times \int_0^{2\pi} \beta_x^{|n_1|/2}\beta_y^{|n_2|/2}e^{i[n_1\mu_x+n_2\mu_y-(\Delta-p)\theta]}\bar{K}\,d\theta
$$

are (i) the factor $\frac{\pi(\Delta-[\Delta])}{\sin[\pi(\Delta-[\Delta])]}$ makes the summed-resonance driving term "sensitive" to the position of the working point with respect to the closest resonance, and (ii) the factor π inside the exponential of the summed-resonance driving term (replacing the angle θ in the single-resonance driving term) makes the summed-resonance driving term dependent on the position where the origin of the coordinate system is established.

Analytic comparison of the influence of single and summed resonances

It is interesting to compare the contribution to the coupling excitation from all resonances to that of the closest single resonance.

Using the thin lens approximation the ith contribution to $C_{n_1,n_2,p}$ can be written

$$
(\Delta C_p)_i \simeq A(\theta_i) \int_{\theta_i}^{\theta_i+\Delta\theta_i} e^{-i(\Delta-p)\theta}\,d\theta
$$
$$
= A(\theta_i)\frac{i}{\Delta-p}e^{-i(\Delta-p)\theta_i}\{\cos[(\Delta-p)\Delta\theta_i]-1-i\sin[(\Delta-p)\Delta\theta_i]\}
$$
$$
\simeq \frac{R^2}{\pi(2R)^{N/2}|n_1|!\,|n_2|!}K_i\Delta\theta_i(\beta_x)_i^{|n_1|/2}(\beta_y)_i^{|n_2|/2}e^{i[n_1(\mu_x)_i+n_2(\mu_y)_i-(\Delta-p)\theta_i]}. \qquad (13)
$$

Figure 1 shows the ratio between $\|(\Delta C_{n_1,n_2,\infty})_i\|$ and $\|(\Delta C_{n_1,n_2,p})_i\|$ versus the distance from the resonance
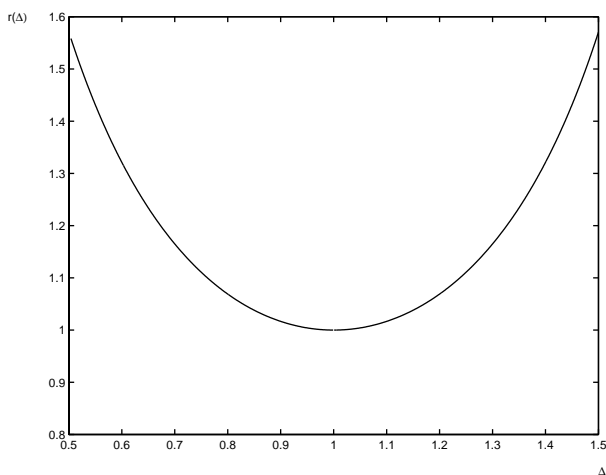

FIG. 1. Ratio $r(\Delta)$ between $\|\Delta C_{n_1,n_2,\infty}\|$ and $\|\Delta C_{n_1,n_2,1}\|$ versus Δ.

---

[5]Note that the phase terms are different even when exactly on resonance.

($[\Delta] = 1$). The formulas (11) and (13) give the same result for the modulus of the driving terms when exactly on resonance. A difference between (11) and (13) increases (circa) quadratically as one moves away from Δ integer. Agreement between the two formalisms can therefore be expected only if the working point is close enough to the resonance to be compensated.[5] However, this is not usually the case if the aim is the full compensation of the linear coupling, that is, both the sum and difference resonances. In most practical cases, the working point is chosen close to the difference resonance and relatively distant from the sum resonance. The following sections are dedicated to pointing out some of the general consequences of the summed-resonance theory.

III. UNCOUPLED LINEAR CASE

A. Closed-orbit distortion from a dipole kick

Equation (11) can be applied to the resonance family

$$
Q_z = p, \qquad (14)
$$

where $z \equiv x, y$. This leads to the expressions for the closed-orbit distortion due to a dipole kick and links the

single-resonance theory [3,8] to the integrated theory of Courant and Snyder [7]. In this case

$$C_\infty = \sum_{p=-\infty}^{+\infty} \int_0^{2\pi} A(\theta)e^{-i(Q_z-p)\theta}\, d\theta\,, \qquad (15)$$

where now [3]

$$A(\theta) = \frac{1}{2^{3/2}\pi R^{1/2}}\sqrt{\beta_z(\theta)}\, e^{i\mu_z(\theta)}\frac{\Delta B}{B\rho}\,, \qquad (16)$$

$\Delta B/B\rho$ is the dipole error. For a localized error of length Δl (thin lens approximation),

$$\begin{aligned}(\Delta C_\infty)_i &= -\frac{1}{2^{3/2}R^{1/2}}\frac{Q_z-[Q_z]}{\sin[\pi(Q_z-[Q_z])]}\sqrt{\beta_z}\frac{\Delta l\Delta B}{B\rho}\,e^{i[\mu_z(\theta)-(Q_z-[Q_z])\pi]}\\ &= -\frac{1}{2^{3/2}R^{1/2}}\frac{Q_z-[Q_z]}{\sin(\pi Q_z)}\frac{\Delta l\Delta B}{B\rho}\sqrt{\beta_z}\,e^{i[\mu_z(\theta)-Q_z\pi]}.\end{aligned} \qquad (17)$$

Comparing Eq. (17) to the closed-orbit distortion (at the origin) due to a kick occurring at a given position θ

$$(z)_{\theta=0} = \frac{\sqrt{\beta_z(0)}}{2\sin(\pi Q_z)}\sqrt{\beta_z(\theta)}\frac{\Delta B\Delta l}{B\rho}\cos[\mu_z(\theta)-\pi Q_z] \qquad (18)$$

shows that the normalized orbit distortion differs from $\text{Re}(\Delta C_\infty)_i$ by only a constant,

$$\left(\frac{z}{\sqrt{\beta_z}}\right)_{\theta=0} \equiv -\frac{1}{(2R)^{-1/2}(Q_z-[Q_z])}\text{Re}(\Delta C_\infty)_i\,. \qquad (19)$$

B. Betatron amplitude modulation

Applying the same procedure to the resonance family

$$Q_z = 2p\,, \qquad (20)$$

one gets the modulation of the betatron function due to a small gradient error occurring at a given position θ. In this case

$$C_\infty \equiv \sum_{p=-\infty}^{+\infty} \int_0^{2\pi} A(\theta)e^{i(2Q_z-p)\theta}\, d\theta\,, \qquad (21)$$

with

$$A(\theta) = \frac{1}{4\pi R}\beta_z(\theta)e^{2i\mu_z(\theta)}\frac{R^2}{B\rho}\frac{\partial B_y}{\partial x}\,. \qquad (22)$$

This gives

$$\begin{aligned}(\Delta C_\infty)_i &= -\frac{1}{2}\frac{Q_z-[Q_z]}{\sin[2\pi(Q_z-[Q_z])]}\beta_z(\theta)\frac{\Delta l}{B\rho}\frac{\partial B_y}{\partial x}\\ &\quad\times e^{i[2\mu_z(\theta)-2(Q_z-[Q_z])\pi]}\\ &= -\frac{1}{2}\frac{Q_z-[Q_z]}{\sin(2\pi Q_z)}\beta_z(\theta)\frac{\Delta l}{B\rho}\frac{\partial B_y}{\partial x}\,e^{i[2\mu_z(\theta)-2Q_z\pi]}.\end{aligned} \qquad (23)$$

The last expression coincides with the modulation of the beta function (at the origin)

$$\begin{aligned}(\Delta\beta_z)_{\theta=0} &= \frac{\beta_z(0)}{\sin(2\pi Q_z)}\beta_z(\theta)\frac{\Delta l}{B\rho}\frac{\partial B_y}{\partial x}\\ &\quad\times\cos\{2[\mu_z(\theta)-Q_z\pi]\}\end{aligned} \qquad (24)$$

and shows that the normalized modulation differs from $\text{Re}(\Delta C_\infty)_i$ by only a constant,

$$\left(\frac{\Delta\beta_z}{\beta_z}\right)_{\theta=0} \equiv -\frac{1}{2^{-1}(Q_z-[Q_z])}\text{Re}(\Delta C_\infty)_i\,. \qquad (25)$$

IV. LINEAR BETATRON COUPLING

Analyses of betatron coupling can be broadly divided into two categories: the matrix approach [10–12] that decouples the single-turn matrix to reveal the normal modes and the Hamiltonian approach [8,13] that evaluates the coupling in terms of the action of resonances using a perturbation method. The latter is often regarded as being less exact but good for physical insight. The general belief is that the correction of the two closest sum and difference resonances to the working point should be sufficient to reduce the off-axis terms in the 4×4 single-turn matrix, but in most cases this is not successful.

A. Matrix method for coupling compensation

The 4×4 single-turn matrix in the presence of skew quadrupoles and/or solenoids is of the form

$$\mathbf{T} = \begin{pmatrix} M & n \\ m & N \end{pmatrix}, \qquad (26)$$

where $M, n, m, N \in \Re^{2\times2}$. Coupling compensation is achieved by setting the two 2×2 matrices n and m to zero. Because of symplecticity and periodicity of $\mathbf{T}$ only four free parameters (that is the strengths of four compensator units) are required. However, this compensation is valid only at the origin of $\mathbf{T}$. A transformation can also be applied to the matrix $\mathbf{T}$ that decouples the linear motion, thus making it possible to describe the beam in the whole machine with the well-known Courant and Snyder parametrization in the transformed coordinates [10].

B. Classical Hamiltonian method for coupling compensation

This method is based on the expansion in a Fourier series of the coupling perturbation term in the Hamiltonian. The standard assumption that only the low-frequency

components significantly influence the motion means, in practice, that only the nearest sum and difference resonances require compensation (single-resonance compensation). The essential differences between this and the matrix approach are (i) the matrix method is exact while the Hamiltonian method is approximate; (ii) a coupling compensation made by the matrix method is valid only at one point in the ring whereas the Hamiltonian method gives a global correction; and (iii) the matrix method leaves finite excitations in all resonances, including those closest to the working point, whereas the Hamiltonian method leaves finite excitations only in the far resonances. The reason for the two last points is that the matrix method includes all resonances automatically and combines them in such a way that the matrix is uncoupled at one point while the Hamiltonian method sets only the closest sum and difference resonances to zero. If the far resonances have little effect, then the two methods are virtually equivalent. This is, however, an uncommon situation. The method outlined in Section II to sum the effect of all the resonances belonging to the same family leads to a correspondence between the standard Hamiltonian method and the matrix method. Once this is done, the natural question is which of the two methods is the better for machine-operation.

V. THE COUPLED HÉNON MAP

In this section, the summed-resonance approach is shown to be equivalent to the matrix approach and both are compared to the single-resonance compensation by performing a numerical analysis on the so-called Hénon map [14]: a hyper-simplified lattice model[6] whose phase-space trajectories show all the fundamental characteristics of a generic (more complicated) map. In this application the linear coupling is generated and corrected by $1 + 4$ thin skew quadrupoles.[7] The global compensation of the coupling resonances (at $\theta = 0$) is achieved if

$$\sum_{j=1}^{5} [\mathrm{Re}(\Delta C_{\infty}^{-}) + i\,\mathrm{Im}(\Delta C-_{\infty})] = 0$$
$$\sum_{j=1}^{5} [\mathrm{Re}(\Delta C_{\infty}^{+}) + i\,\mathrm{Im}(\Delta C+_{\infty})] = 0. \tag{27}$$

The compensation for both the sum and the difference resonance is obtained solving the four-equations system (for the four unknown k_i) given by (27).

Table I shows a comparison between the strengths of the four correctors (k_{2-5}) when compensating the single-turn matrix, the two infinite families of sum and difference

TABLE I. Compensator strengths (k_{2-5}) in the presence of the coupling source k_1 using the single-turn matrix compensation and the summed- and single-resonance compensations.

k (m^{-2})	Matrix	Summed	Single
k_1 (source)	0.5	0.5	0.5
k_2	-0.051	-0.050	0.559
k_3	0.034	0.033	0.554
k_4	-0.319	-0.313	0.476
k_5	-0.275	-0.275	0.117

resonances (for the same $\theta = 0$), and the closest sum and difference resonances to the working point. The single-turn matrix compensation has been performed by means of the MAD program [15] while the (single- and multiple-) resonance compensation has been obtained making use of the AGILE program [16] in which the formula (11) has been implemented. The single-turn matrix (at $\theta = 0$) in presence of the coupling source $k_1 = 0.5$ m^{-2} (no compensation) has nonzero off-axis 2×2 submatrices given by

$$\mathbf{T} = \begin{pmatrix} M & n \\ m & N \end{pmatrix} = \begin{pmatrix} & & 0.49 & 0.49 \\ & & 0.02 & 0.02 \\ -0.23 & -0.24 & & \\ -0.01 & -0.01 & & \end{pmatrix}, \tag{28}$$

while the residual values of n and m after the single-resonance compensation ($C+ = C- = 0$) are given by

$$\mathbf{T} = \begin{pmatrix} & & -0.11 & -4.67 \\ & & 0.02 & 0.15 \\ 0.03 & -4.57 & & \\ 0.03 & -0.09 & & \end{pmatrix}. \tag{29}$$

The off-axis terms are in fact larger after the compensation then before. This is explained by the influence of the far resonances that cannot be neglected in this case. The same thing can be concluded by looking at the driving terms of the closest sum and difference resonances before the correction

$$|C^+| = 0.0628, \qquad |C^-| = 0.0628, \tag{30}$$

and after correction by the matrix method

$$|C^+| = 0.0207, \qquad |C^-| = 0.1018. \tag{31}$$

The last two equations show that the far sum and difference resonances have a "weight" comparable (bigger in the case of the difference resonance) with the nearly resonances. The virtually perfect agreement for the correction strengths for the matrix and summed-resonance approaches implies a complete equivalence of the methods and confirms the importance of the far resonances. The quantitative

---

[6]A linear lattice model containing only one sextupolar kick.

[7]Lattices with only solenoids or with both types of coupling elements give the same kinds of results.

difference between the two approaches can be better investigated by means of a tracking analysis. In the following, the results from stability and frequency diagrams as well as the calculation of the dynamic aperture for the compensated Hénon map are shown.

A. Stability analysis through tracking

A stability diagram can be obtained by the following procedure: for each initial condition inside a given grid in the physical plane (x, y) $(p_x = p_y = 0)$, the symplectic map representing the lattice is iterated over a certain number of turns. If the orbit is still stable after the last turn, the nonlinear tunes can be calculated using one of the methods described in [17,18]. In the stability diagram the stable initial conditions are plotted.

Figures 2–4 show the stability diagrams, first for the uncoupled Hénon map and then for the coupled Hénon map after the single-resonance compensation and after the summed-resonance compensation. The comparison points out that the summed-resonance compensation allows a more efficient restoration of the uncoupled optics. It is significant that the analysis of the degree of excitation is relative to the resonances $(3, -6)$, $(1, -4)$, and $(2, -5)$ for the two different compensation approaches.

Using the perturbative tools of normal forms [19] one can calculate the value of the first resonant coefficient (leading term) in the interpolating Hamiltonian for the considered resonances. The leading term can be considered as a "measure" of the resonance excitation. It can be shown [20] that in absence of coupling the leading term
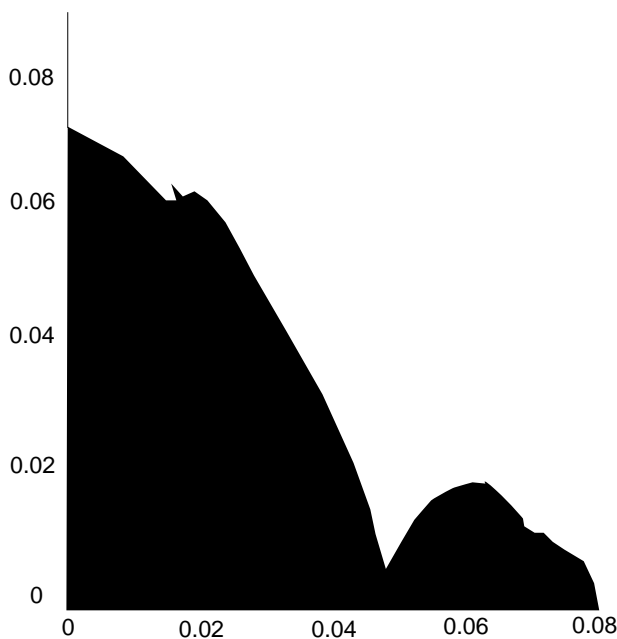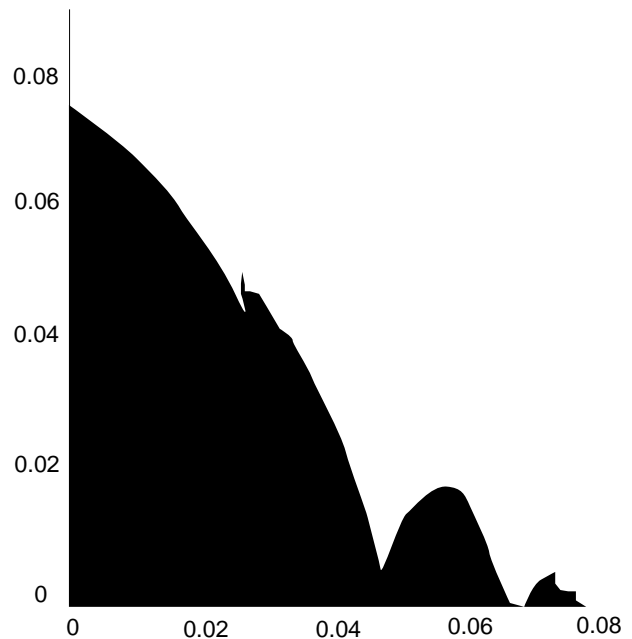

FIG. 3. Stability domain after the summed-resonance compensation.

of the resonances $(3, -6)$ and $(1, -4)$ is different from zero (first order excitation) whereas the leading term of the resonance $(2, -5)$ is zero (second order excitation). The strength of the coupling (that is, in the considered case, the strength of the residual coupling after the compensations) is proportional to the growth of the leading term of the first order nonexcited resonances and to the decrease of the leading term of the other ones. The resonance

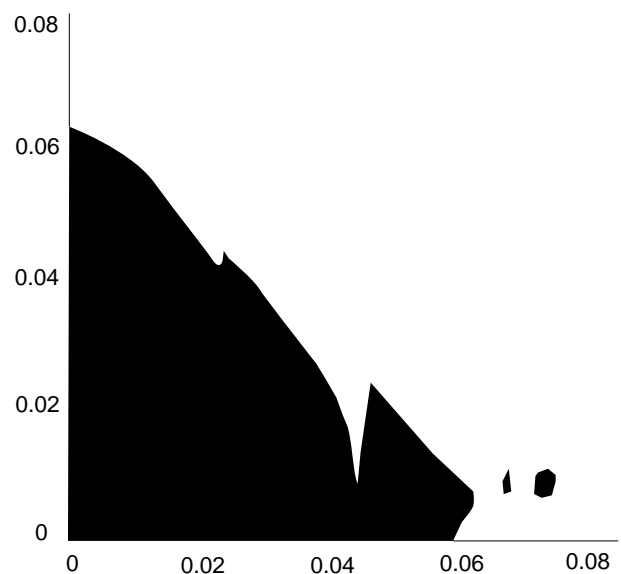FIG. 2. Stability domain of the uncoupled Hénon map.

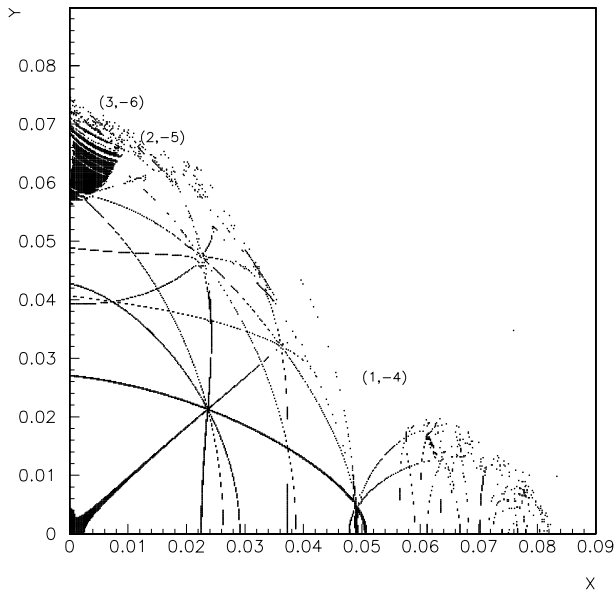FIG. 4. Stability domain after the single-resonance compensation.

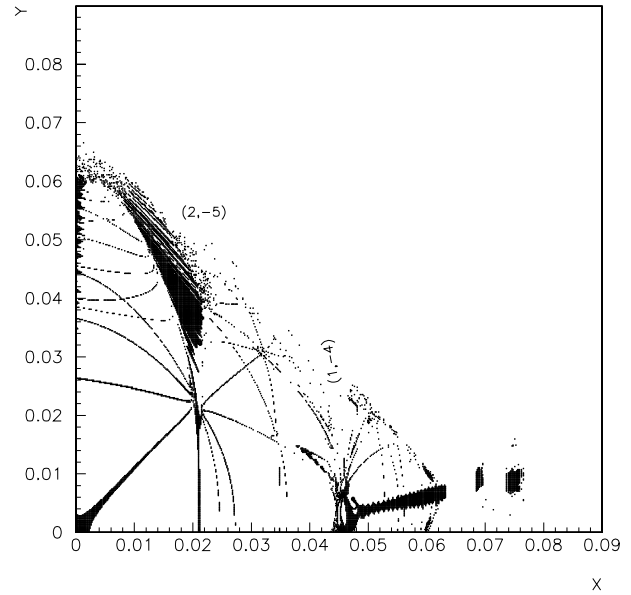FIG. 5.   Network of resonances of the uncoupled Hénon map.

FIG. 7.   Network of resonances after the single-resonance compensation.

degree of the excitation varying the compensation approach can be better visualized plotting the network of the resonances and their widths inside the stability domain. The analysis of Figs. 5–7 confirms that the single-resonance method is characterized by a residual coupling considerably stronger than the one left by the summed-resonance compensation.
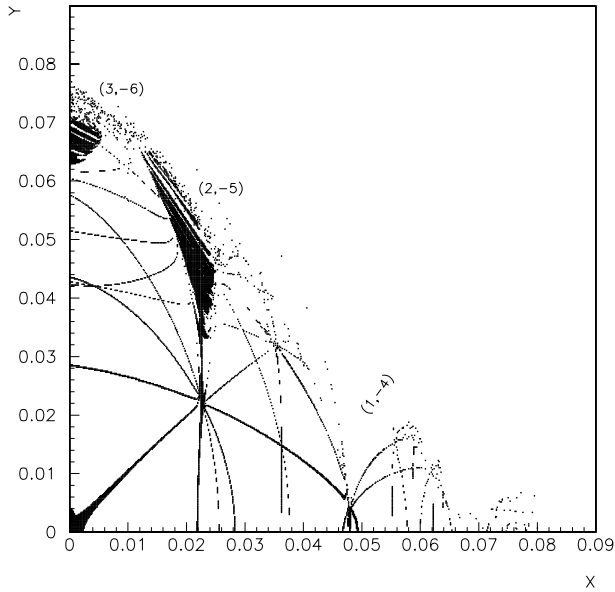

FIG. 6.   Network of resonances after the summed-resonance compensation.

B. Dynamic aperture calculations

The dynamic aperture as a function of the number of turns N can be defined [21] as the first amplitude where particle loss occurs, averaged over the phase space. Particles are started along a grid in the physical plane (x, y):

$$x = r \cos \theta, \qquad y = r \sin \theta, \qquad (32)$$

and initial momenta p_x and p_y are set to zero. Let $r(\theta, N)$ be the last stable initial condition along θ before the first loss (at a turn number lower than N). The dynamic aperture is defined as

$$D = \left\{ \int_0^{\frac{\pi}{2}} [r(\theta, N)]^4 \sin(2\theta) \, d\theta \right\}^{1/4}. \qquad (33)$$

An approximated formula for the error associated to the discretization over both the radial and the angular coordinate can be obtained by replacing the dynamic aperture definition with a simple average over θ. Using a Gaussian sum in quadrature the associated error reads

$$\Delta D = \sqrt{ \frac{(\Delta r)^2}{4} + \left\langle \left| \frac{\partial r}{\partial \theta} \right| \right\rangle^2 \frac{(\Delta \theta)^2}{4} }, \qquad (34)$$

where Δr and $\Delta \theta$ are the step sizes in r and θ, respectively. In Table II the values (with the associated errors) of the dynamic aperture are quoted for the three studied optics for short ($N = 5000$) and medium ($N = 20\,000$) term tracking.

The difference between the summed- and the single-resonance compensations is noticeable: the compensation of the all families relative to the coupling resonances allows an improvement close to 10% with respect to the

TABLE II. Dynamic aperture values relative to the uncoupled Hénon map and after the summed- and single-resonance compensations. The associated error [according to the formula (34)] is about 2% for $N = 5000$ and about 4% for $N = 20\,000$.

D (m)	Uncoupled	Summed	Single
$N = 5000$	0.041	0.041	0.037
$N = 20\,000$	0.041	0.041	0.037

case in which the high frequency part of the perturbative Hamiltonian is neglected.

VI. CONCLUSIONS

A general method has been derived for the summation of all the resonances within a given family both for the linear and for the nonlinear cases. The fact that this summation is valid and gives a meaningful result is confirmed by its application to the known closed-orbit distortion equation, the betatron-modulation equation, and the decoupling of the linear transfer matrix for a ring. The application of the summed-resonance driving term to the coupling raises the question of the relative merits of the different types of coupling compensation that are now possible. This problem has been investigated with the help of the Hénon map. The results indicate that the summed-resonance compensation (equivalent to the matrix approach) is the more beneficial for the dynamic aperture.

ACKNOWLEDGMENTS

[1] R. Hagedorn, Report No. CERN 57-1, 1957.
[2] A. Schoch, Report No. CERN 57-23, 1957.
[3] G. Guignard, Report No. CERN 76-06, 1976.
[4] N. Merminga and K. Y. Ng, Fermilab Report No. FN-493, 1988.
[5] H. G. Hereward, in Proceedings of the Fifth International Conference on High Energy Accelerators, Dubna, 1963 (unpublished).
[6] G. Guignard, in *Nonlinear Dynamics and the Beam-Beam Interaction,* edited by M. Month and J. C. Herrera, AIP Conf. Proc. No. 57 (AIP, New York, 1980), pp. 69–83.
[7] E. D. Courant and H. S. Snyder, Ann. Phys. (Paris) **3**, 1 (1958).
[8] G. Guignard and J. Hagel, Report No. CERN 92-01, 1992.
[9] I. S. Gradshteyn and I. M. Ryzhik, *Table of Integrals, Series and Products* (Academic Press, London, 1980).
[10] D. Edwards and L. Teng, IEEE Trans. Nucl. Sci. **20**, 885 (1973).
[11] R. Talman, "Coupled betatron motion and its compensation", US-CERN School of Particle Accelerators, Capri, Italy, 1988 (unpublished).
[12] S. Peggs, in *Proceedings of the Particle Accelerator Conference, 1983* [IEEE Trans. Nucl. Sci. **30**, 2460 (1983)].
[13] P. J. Bryant, Report No. CERN 94-01, 1994.
[14] M. Henon, Appl. Math. **27**, 291–312 (1969).
[15] The MAD program, H. Grote and F. C. Iselin, Report No. CERN/SL/90-13, 1990.
[16] AGILE-lattice program, P. J. Bryant, available at http://nicewww.cern.ch/~bryant (unpublished).
[17] R. Bartolini, M. Giovannozzi, W. Scandale, A. Bazzani, and E. Todesco, in *Proceedings of the 5th European Particle Accelerator Conference, Barcelona, Spain, 1996* (Institute of Physics, Bristol, UK, 1996), Vol. II, p. 1329.
[18] J. Laskar, C. Floschele, and A. Celletti, Physica (Amsterdam) **56D**, 253 (1992).
[19] A. Bazzani, G. Servizi, E. Todesco, and G. Turchetti, Report No. CERN 94-02, 1994.
[20] G. De Ninno and E. Todesco, Phys. Rev. E **55**, 2059–2062 (1997).
[21] E. Todesco and M. Giovannozzi, Phys. Rev. E **53**, 4067 (1996).
[22] P. J. Bryant and K. Johnshen, *The Principles of Circular Accelerators and Storage Rings* (Cambridge University Press, Cambridge, England, 1993.
[23] D. C. Carey, *The Optics of Charged Particles Beams* (Harwood Academic Publishers, Chur, Switzerland, 1987).